Articles

Thermally Reversible Photochemical Haptotropic Rearrangement of Diiron Carbonyl Complexes Bearing a Bridging Acenaphthylene or Aceanthrylene Ligand

Shota Niibayashi,[‡] Kouki Matsubara,[†,§] Masa-aki Haga,[⊥] and Hideo Nagashima*[,†,‡,§]

Institute for Materials Chemistry and Engineering, Graduate School of Engineering Sciences, and CREST, Japan Science and Technology Corporation (JST), Kyushu University, Kasuga, Fukuoka 816-8580, Japan, and Department of Applied Chemistry, Chuo University, Kasuga, Bunkyo-ku, Tokyo, Japan

Received August 18, 2003

The haptotropic rearrangement of diiron carbonyl species on the conjugate π-ligand in (μ_2,η^3:η^5-acenaphthylene)$Fe_2(CO)_5$ (**1**) and its analogue (μ_2,η^3:η^5-aceanthrylene)$Fe_2(CO)_5$ (**2**) is investigated in both solution and solid states. The diiron complexes **1** and **2** have two isomers, and each isomer is isolated and characterized. Isomers **1-A** and **2-A** are thermodynamically more stable than **1-B** and **2-B**, respectively ($\Delta G°_{296} = 2.3$ kcal/mol for **1**; $\Delta G°_{296} > 2.3$ kcal/mol for **2**). The thermodynamically less stable isomers can be prepared photochemically. Interconversions between **1-A** and **1-B** and between **2-A** and **2-B** occur both thermally and photochemically. Kinetic studies on the thermal isomerizations in solution provide $\Delta G^{‡}_{298} = 23 \pm 1$ kcal/mol, $\Delta H^{‡}_{298} = 23 \pm 1$ kcal/mol, and $\Delta S^{‡}_{298} = 1 \pm 4$ cal/mol·deg for the reaction of **1-B** to **1-A**, and $\Delta G^{‡}_{298} = 26 \pm 1$ kcal/mol, $\Delta H^{‡}_{298} = 26 \pm 1$ kcal/mol, and $\Delta S^{‡}_{298} = 0 \pm 2$ cal/mol·deg for the reaction of **2-B** to **2-A**. Photochemical interconversion at $\lambda = 600$ nm provides the isomer ratio of **1-A**:**1-B** = 9:91 at the photostatic state, and **2-A**:**2-B** = 66:34. In both of the isomerization reactions, irradiation with light of shorter wavelength tends to give lower ratios of the thermodynamically less stable isomers. The quantum yields of the isomerization reactions are found to be $\Phi_{\mathbf{1-A}\rightarrow\mathbf{1-B}} = 0.30(3)$, $\Phi_{\mathbf{1-B}\rightarrow\mathbf{1-A}} = 0.09(1)$, $\Phi_{\mathbf{2-A}\rightarrow\mathbf{2-B}} = 0.013(2)$, and $\Phi_{\mathbf{2-B}\rightarrow\mathbf{2-A}} = 0.009(1)$. From these experimental data the reaction mechanisms of the thermal and photochemical haptotropic rearrangements are discussed with the aid of EHMO calculations. A single crystal of **1-B** converts to a single crystal of **1-A** upon heating. A photolysis (5 min by a 500 W xenon lamp)/thermal treatment (10 min at 100 °C) cycle of a KBr pellet containing **1-A** or **1-B** results in reversible interconversion between **1-A** and **1-B** in the solid state, which can be monitored by the IR absorption at $\nu = 1825$ cm^{-1}. The cycle is repeatable for over 10 times without change in the signal intensity. These results are the first to indicate a possible organometallic photochromism in the solid state detectable by the IR light.

Introduction

Reversible structural changes of a single molecule induced by photolysis have the potential to develop underlying principles of molecular switches.[1] Organic photochromic molecules are one successful example of this issue, and a number of studies have been undertaken to date.[2] In contrast, there are only a few organometallic compounds that undergo reversible photoisomerization or thermally reversible photoisomerization between their two possible structural isomers.[3] A recent proposal by Burger and co-workers, who reported on photochromic diruthenium complexes, raises the possible utility of dinuclear organometallic complexes for thermo-optical switches; photolysis of a yellow-orange isomer resulted in the formation of a ther-

* Corresponding author. E-mail: nagasima@cm.kyushu-u.ac.jp.
† Institute for Materials Chemistry and Engineering, Kyushu University.
‡ Graduate School of Engineering Sciences, Kyushu University.
§ CREST, Japan Science and Technology Corporation, Kyushu University.
⊥ Chuo University.

(1) Feringa, B. L. *Molecular Switches*; Wiley: New York, 2001.

(2) Reviews on organic photochromic compounds: (a) Dürr, H.; Bouas-Laurent, H. *Photochromism*; Elsevier: Amsterdam, 1990. (b) Crano, J. C.; Guglielmetti, R. J. *Organic Photochromic and Thermochromic Compounds Vol. 1 and 2*; Kluwer Academic/Plenum: New York, 1999. (c) Wayne, R. P. *Principles and Applications of Photochemistry*; Oxford: 1988. (d) Irie, M. *Chem. Rev.* **2000**, *100*, 1685.

(3) (a) Burger, P. *Angew. Chem., Int. Ed.* **2001**, *40*, 1917. (b) Boese, R.; Cammack, J. K.; Matzger, A. J.; Pflug, K.; Tolman, W. B.; Vollhardt, K. P. C.; Weidman, T. W. *J. Am. Chem. Soc.* **1997**, *119*, 6757. (c) Adams, R. D.; Cortopassi, J. E.; Aust, J.; Myrick, M. *J. Am. Chem. Soc.* **1993**, *115*, 8877. (d) Ogino, H.; Yuki, M.; Okazaki, M.; Inomata, S. *Angew. Chem., Int. Ed.* **1998**, *37*, 2126. (e) Kawano, Y.; Tobita, H.; Ogino, H. *Organometallics* **1992**, *11*, 499.

10.1021/om034117i CCC: $27.50
Publication on Web 01/10/2004

Scheme 1

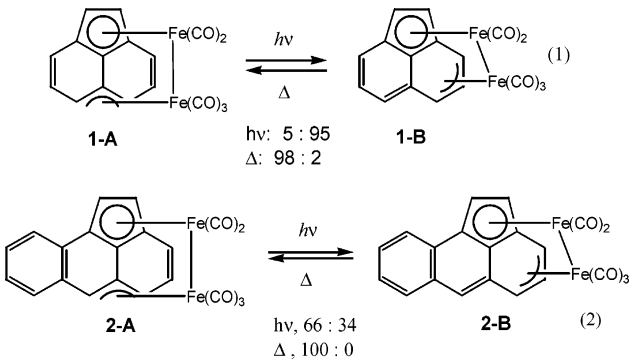

modynamically less stable colorless isomer, which regenerated the initial isomer by releasing 11 kcal/mol of energy.[3a] Several earlier examples, which can be regarded as a type of "thermo-optical switch", were reported in context with organometallic light-harvesting systems[3b−d] and in relation to thermally and photochemically induced structual isomerization of dinuclear metal carbonyls.[3e]

We have been interested in the posslibity of thermally reversible photoisomerization involving the haptotropic rearrangement. Many studies on the thermal haptotropic rearrangement of metal carbonyls bound to polyaromatic hydrocarbons or polyenes have been carried out both experimentally and theoretically;[4−6] however, little is known about the photochemical haptotropic rearrangement.[7a,b] In 1991 we reported the rearrangement between two isomers of a dinuclear iron complex [(μ_2,η^3:η^5-acenaphthylene)$Fe_2(CO)_5$] (**1**), as shown in Scheme 1, eq 1.[8] Although possible rearrangement from **1-A** to **1-B** had already been excluded by Churchill and co-workers in the early 1970s,[9] C_s-symmetric **1-A** is eventually converted to the unsymmetrical isomer **1-B** upon photoirradiation of its solution. The novel isomer **1-B** is thermodynamically less stable than **1-A**, and a thermal reverse reaction from **1-B** to **1-A** occurs when a solution of **1-B** is allowed to stand in the dark. Further experiments revealed that both the thermal and photochemical rearrangements are essentially reversible; however, the isomer ratio in the thermal equilibrium (**1-A**:**1-B** = 98:2) is substantially different from that at the photostatic state (**1-A**:**1-B** = 5:95). In further investigations of the systems analogous to **1-A**, rearrangements of (μ_2,η^3:η^5-guaiazulene)$Fe_2(CO)_5$, (μ_2,η^3:η^5-guaiazulene)$Ru_2(CO)_5$, and (μ_2,η^3:η^5-guaiazulene)-$M_2(CO)_4L$ (M = Fe, Ru; L = phosphines and phosphites, isonitriles) were studied, in which interconversion between two haptotropic isomers of the complexes takes place both thermally and photochemically.[10,11] Although detailed investigations of these systems have made clear the effects of metals (Fe[10a] or Ru[10b]) and ligands (CO,[10a] phosphorus ligands,[10b] and isocyanides[10c]) on the thermal and photochemical haptotropic rearrangements, in all cases the isomer ratios of the photochemical processes are not very different from those of the thermal processes. This was not satisfactory to look at mechanistic differences in the photochemical and the thermal processes, prompting us to reinvestigate the thermal and photochemical haptotropic rearrangements of [(μ_2,η^3:η^5-acenaphthylene)$Fe_2(CO)_5$] (**1**).

In this paper, we wish to report the detailed studies on the thermal and photochemical haptotropic rearrangements between **1-A** and **1-B** in both solution and the solid state. The novel aceanthrylene homologues, [(μ_2,η^3:η^5-aceanthylene)$Fe_2(CO)_5$], **2-A** and **2-B**, were synthesized to better understand various factors of the rearrangement. In solution, we determined the thermal equilibrium ratios at different temperatures and carried out kinetic studies, from which $\Delta H^{\ddagger}$ and $\Delta S^{\ddagger}$ were calculated. Wavelength dependency and quantum yields of the photochemical process were also investigated in solution. Mechanistic considerations were made from these data with the aid of structural features of **1-A**, **1-B**, **2-A**, and **2-B** and EHMO calculations of the rearrangement of **1**.

Apart from the rearrangement in solution, we have found that the thermal reaction from **1-B** to **1-A** occurs in a single crystal, whereas both the photochemical rearrangement from **1-A** to **1-B** and the reverse thermal pathway from **1-B** to **1-A** can be accomplished in a solid sample dispersed in a KBr pellet. Although the thermal haptotropic rearrangement of organonickel complexes has already been investigated in the solid state,[12] to our knowledge there has been no report on the thermally reversible photoisomerization of one haptotropic isomer to another in the solid state. The thermal structural change from **1-B** to **1-A** in the single crystal described in this paper could be shown by X-ray crystallography, while the thermally reversible photoisomerization be-

(4) For reviews: (a) Mann, B. E. In *Comprehensive Organometallic Chemistry*; Wilkinson, G., Stone, F. G. A., Abel, E. W., Eds.; Pergamon: Oxford, 1982; Vol. 3, Chapter 20. (b) Mann, B. E. *Chem. Soc. Rev.* **1986**, *15*, 167. (c) Degenello, G. *Transition Metal Complexes of Cyclic Polyolefins*; Academic Press: London, 1982.

(5) Representative examples for the haptotropic rearrangement of mononuclear transition metal complexes: (a) Treichel, P. M.; Johnson, J. W. *Inorg. Chem.* **1977**, *16*, 749. (b) Kirss, R. U.; Treichel, P. M. *J. Am. Chem. Soc.* **1986**, *108*, 853. (c) Rerek, M. E.; Basolo, F. *Organometallics* **1984**, *3*, 647. (d) Ustynyuk, N. A.; Novikova, L. N.; Oprunenko, Y. F.; Malyugina, S. G.; Ustynyuk, Y. A. *J. Organomet. Chem.* **1984**, *277*, 75. (e) Nakasuji, K.; Yamaguchi, M.; Murata, I. *J. Am. Chem. Soc.* **1986**, *108*, 325. (r) Veiros, L. F. *J. Organomet. Chem.* **1999**, *587*, 221. (g) Trifonova, O. I.; Ochertyanova, E. A.; Akhmedov, N. G.; Roznyatovsky, V. A.; Laikov, D. N.; Ustynyuk, N. A.; Ustynyuk, Y. A. *Inorg. Chim. Acta* **1998**, *280*, 328. (h) Oprunenko, Y. F.; Akhmedov, N. G.; Laikov, D. N.; Malyugina, S. G.; Mstislavsky, V. I.; Roznyatovsky, V. A.; Ustynyuk, Y. A.; Ustynyuk, N. A. *J. Organomet. Chem.* **1999**, *583*, 136. (i) Fryzuk, M. D.; Jafarpour, L.; Kerton, F. M.; Love, J. B.; Rettig, S. J. *Angew. Chem., Int. Ed.* **2000**, *39*, 767. (j) Oprunenko, Y.; Malyugina, S.; Vasil'ko, A.; Lyssenko, K.; Elschenbroich, C.; Harms, K. *J. Organomet. Chem.* **2002**, *641*, 208.

(6) (a) Silvestre, J.; Albright, T. A. *J. Am. Chem. Soc.* **1985**, *107*, 6829. (b) Albright, T. A.; Hofmann, P.; Hoffmann, R.; Lillya, C. P.; Dobosh, P. A. *J. Am. Chem. Soc.* **1983**, *105*, 3396.

(7) (a) Hughes, R. P.; Carl, R. T.; Hemond, R. C.; Samkoff, D. E.; Reingold, A. L. *J. Chem. Soc., Chem. Commun.* **1986**, 306. (b) King, J. A., Jr.; Vollhardt, K. P. C. *J. Organomet. Chem.* **1989**, *369*, 245.

(8) Nagashima, H.; Fukahori, T.; Itoh, K. *J. Chem. Soc., Chem. Commun.* **1991**, 786.

(9) Churchill, M. R.; Wormald, J. *Inorg. Chem.* **1970**, *9*, 2239.

(10) (a) Nagashima, H.; Fukahori, T.; Nobata, M.; Suzuki, A.; Nakazawa, M.; Itoh, K. *Organometallics* **1994**, *13*, 3427. (b) Matsubara, K.; Oda, T.; Nagashima, H. *Organometallics* **2001**, *21*, 881. (c) Matsubara, K.; Mima, S.; Oda, T.; Nagashima, H. *J. Organomet. Chem.* **2002**, *650*, 96.

(11) There are also a number of examples of the thermal haptotropic isomerization on dinuclear complexes; however, the photoinduced rearrangement of such compounds had not been known until our communication.[8] For an example of the thermal haptotropic rearrangement on dinuclear complex: Cotton, F. A.; Marks, T. J. *J. Organomet. Chem.* **1969**, *19*, 237.

(12) (a) Boese, R.; Stanger, A.; Stellberg, P.; Shazar, A. *Angew. Chem. Int. Ed. Engl.* **1993**, *32*, 1475. (b) Benn, R.; Mynott, R.; Topalović, I.; Scott, F. *Organometallics* **1989**, *8*, 2299. (c) Oprunenko, Y.; Gloriozov, I.; Lyssenko, K.; Malyugina, S.; Mityuk, D.; Mstislavsky, V.; Günther, H.; von Firks, G.; Ebener, M. *J. Organomet. Chem.* **2002**, *656*, 27.

Scheme 2

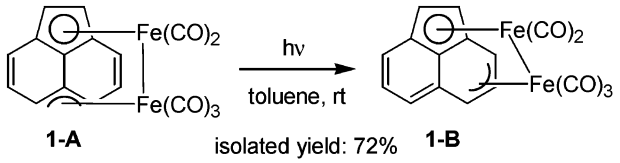

Scheme 3

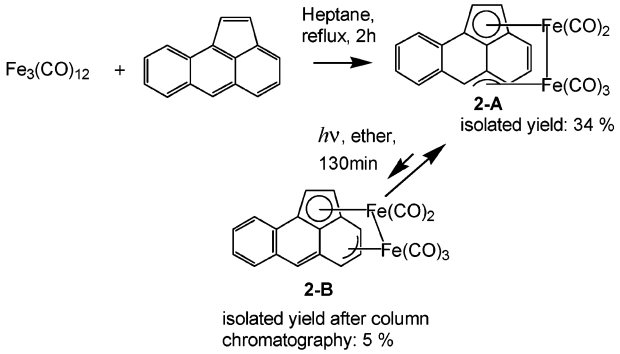

tween **1-A** and **1-B** in KBr pellets could be determined from IR data. These results provide the first experimental evidence that thermally reversible photoisomerization between two haptotropic isomers actually occurs in the solid state. The finding indicates potential to thermo/opt switch capability of this system monitored by IR light.[13]

Results and Discussion

Isolation of Two Isomers of Diiron Complexes 1 and 2. The symmetrical isomer of [(μ_2,η^3:η^5-acenaphthylene)$Fe_2(CO)_5$] (**1-A**) was synthesized according to the method reported by King.[14] As briefly reported in our preliminary communication,[8] a thermodynamically less stable isomer, **1-B**, was formed by photoirradiation of **1-A** in solution. After irradiation of the solution of **1-A** for 1 h in a vacuum-sealed tube with a 400 W high-pressure Hg lamp or a 500 W xenon lamp or by exposure of the solution to sunlight for 1−2 h, **1-B** was formed in nearly quantitative yield based on ^{1}H NMR spectra. Although slow regeneration of **1-A** from **1-B** occurs in solution in the dark, **1-B** is stable in the solid state at room temperature (vide infra). Thus, carefully cooling a toluene solution of **1-B**, generated by photoirradiation of **1-A**, at −78 °C afforded dark red prismatic crystals of pure **1-B** (Scheme 2). A homologous diiron complex bound to aceanthrylene was prepared by a similar procedure; the reaction of [$Fe_3(CO)_{12}$] with aceanthrylene in refluxing *n*-heptane afforded selectively a thermally stable isomer of [(μ_2,η^3:η^5-aceanthrylene)$Fe_2(CO)_5$], **2-A**, in good yield. Since the semistable isomer **2-B** did not isomerize to **2-A** at ambient temperature even in solution (Scheme 1, eq 2), separation of **2-B** from the mixture of **2-A** and **2-B** (**2-A**:**2-B** = 66:34) was achieved by careful column chromatography on alumina at −78 °C (Scheme 3).

The spectral data (^{1}H and ^{13}C NMR and IR) of **1-A**, **1-B**, **2-A**, and **2-B** are listed in Table 1. All of these products were completely assigned with the aid of NOE experiments. The NMR spectrum of **1-B** shows eight ^{1}H and twelve ^{13}C resonances due to the acenaphthylene ligand. The ^{1}H signals due to H1−H5 and the ^{13}C peaks due to C1−C5 appear at a higher region (H1−H5: 2.54−5.31; C1−C5: 57.53−83.59 ppm) than those due to the olefinic group (H6−H8: 5.50−6.13; C6−C8: 114.07−131.78 ppm). These results suggest that the diiron moiety is bonded to C1−C5 carbons. Similar shift to higher field of ^{1}H and ^{13}C resonances in the acenaphthylene and aceanthrylene ligand in **1-A**, **2-A**, and **2-B** (Table 1) is a good indication of the coordination, suggesting the molecular structures shown in Scheme 1. Of importance is the existence of C_s-symmetry in the structure of **1-A**, which shows a simpler NMR pattern than **1-B**.

The existence of an $Fe_2(CO)_5$ moiety can be ascertained from IR and ^{13}C NMR spectra. In **1-B** five IR absorption bands due to the five carbonyl ligands were observed at 2027, 1982, 1961, 1932, and 1856 cm^{-1}, respectively. A particular feature of the IR spectrum of **1-B** (KBr) is the appearance of a weak broad band at 1856 cm^{-1} due to a semibridging carbonyl ligand in

Table 1. ^{1}H, ^{13}C NMR, and IR Data for 1-A, 1-B, 2-A, and 2-B

		1-A	**2-A**	**1-B**	**2-B**
			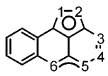		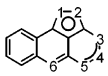
^{1}H NMR (δ)[a]	H1	-	5.92 (d)	4.35 (d)	5.54 (d)
	H2	4.79 (s)	5.77 (d)	3.35 (d)	4.26 (d)
	H3	5.49 (d)	6.26 (d)	5.31 (d)	5.90 (d)
	H4	5.60 (dd)	6.33 (dd)	4.98 (dd)	5.80 (dd)
	H5	4.14 (d)	4.82 (d)	2.54 (d)	3.71 (d)
	H6	-	4.89 (s)	6.08 (s)	6.32 (s)
^{13}C NMR (δ)[a]	C1	-	77.10	71.56	70.07
	C2	78.18	78.84	71.62	69.83
	C3	116.30	117.00	57.53	54.67
	C4	128.92	128.03	83.59	83.01
	C5	57.42	59.37	58.26	60.67
	C6	-	56.82	114.07	114.67
	CO[b]	218.61 (2C)	218.15 (1C)	220.9 (1C)	219.15 (1C)
		216.52 (2C)	217.20 (1C)	216.7 (3C)	215.66 (3C)
		209.18 (1C)	217.13 (1C)	215.8 (1C)	214.55 (1C)
			216.25 (1C)		
			209.68 (1C)		
IR (KBr, cm^{-1})	ν(CO)	2025, 2017,	2035, 1994,	2027, 1982,	2022,
		1964, 1950,	1978, 1960,	1961, 1932,	1920
		1921	1953	1856	

[a] ^{1}H: Measured in C_6D_6 (for **1**) and $CDCl_3$ (for **2**). ^{13}C: Measured in $CDCl_3$ (for **1-A** and **2**) and toluene-d_8 (for **1-B**). [b] Measured in toluene-d_8 at −60 °C (**2-A**) or −80 °C (**1** and **2-B**).

(13) (a) Uchida, K.; Saito, M.; Murakami, A.; Nakamura, S.; Irie, M. *Adv. Mater.* **2003**, *15*, 121. (b) Stellacci, F.; Bertarelli, C.; Toscano, F.; Gallazzi, M. C.; Zerbi, G. *Chem. Phys. Lett.* **1999**, *302*, 563.

(14) King, R. B.; Stone, F. G. A. *J. Am. Chem. Soc.* **1960**, *82*, 4557.

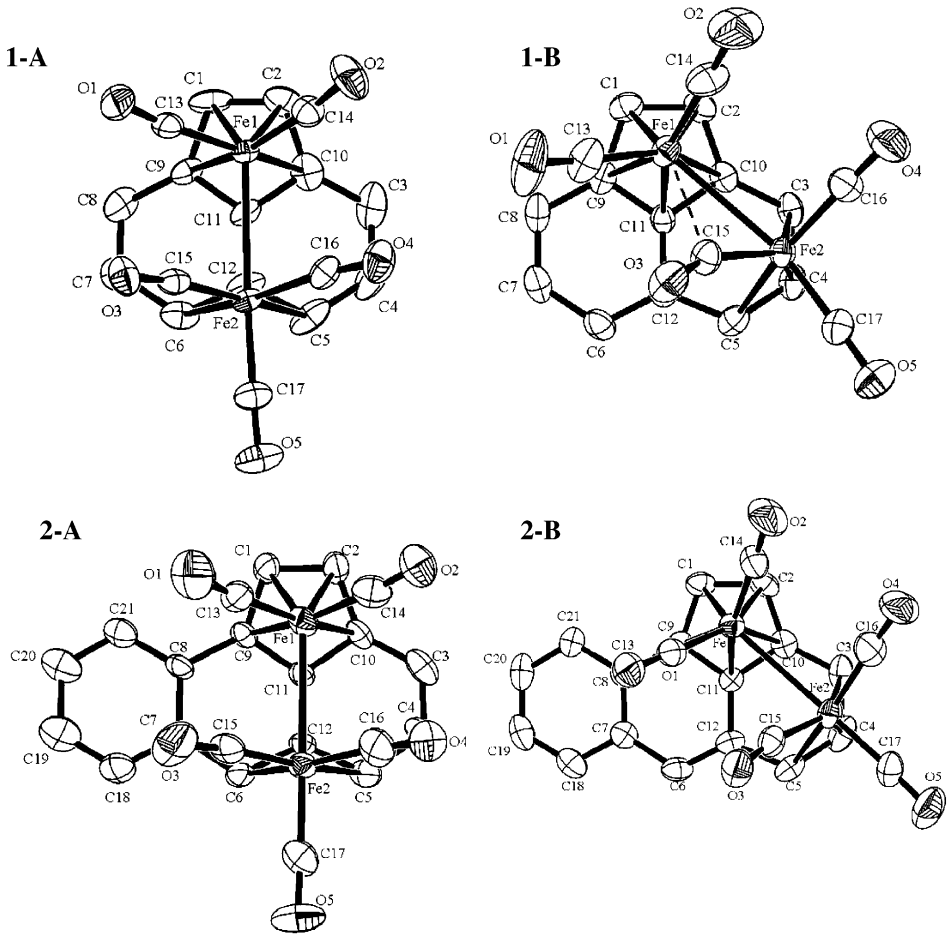

Figure 1. ORTEP drawings of **1-A**, **1-B**, **2-A**, and **2-B** with 50% probability thermal ellipsoids.

1-B,[15] which is not seen in the IR spectrum of **1-B** measured in a CH_2Cl_2 solution. A semibridging CO ligand could not be seen in **1-A**, **2-A**, or **2-B** in both solution and solid states. This suggests that fast site exchange processes of the three CO ligands of the $Fe(CO)_3$ moiety occur in **1-B** in solution.[16] Only three ^{13}C resonances due to the $Fe_2(CO)_5$ moiety in **1-B** are visible at δ 220.9, 216.7, and 215.8 in a 1:3:1 ratio at a temperature range of −80 to 0 °C. Similar CO scrambling processes are seen in all the diiron complexes described in this paper.[17]

Structural determination of all four complexes **1-A**, **1-B**, **2-A**, and **2-B** was performed by crystallography, and the ORTEP drawings, crystallographic data, and representative bond distances and angles are summarized in Figure 1 and Tables 2−6. The crystallography of **1-A** was reported in the early literature;[9] we carried out the analysis again and found some differences in space groups and atomic coordinates. The molecular structures of these four complexes are in accord with those determined from the spectroscopic data. Thus, the iron moieties $Fe(CO)_3$ and $Fe(CO)_2$ are bound to the acenaphthylene ligand in a $\mu_2,\eta^3{:}\eta^5$-coordination mode, in which the C(5), C(12), and C(6) carbons in **1-A** are bonded to the $Fe(CO)_3$ moiety in a η^3-allyl coordination mode. This is in sharp contrast to the coordination in **1-B**, where the C(3), C(4), and C(5) carbons are bonded to the $Fe(CO)_3$ group. In other words, photolysis of **1-A** results in a haptotropic shift of the $Fe(CO)_3$ group from C(5)−C(12)−C(6) to C(3)−C(4)−C(5). Orientation of the η^3-allyl group is *endo* in **1-A**, whereas it is *exo* in **1-B**. There are two isolated carbon−carbon double bonds [C(3)−C(4), C(7)−C(8)] in **1-A**, whereas **1-B** contains a conjugated diene system [C(12)−C(6)−C(7)−C(8)] (Tables 3, 4). The acenaphthylene ligand in **1-A** and **1-B** is not planer; this is attributed to the arrangement of the η^5-Cp moiety and the η^3-allyl moiety, which are coordinated to each Fe atom of the diiron moiety in maintaining the Fe−Fe bond distance of 2.77−2.80 Å. As described above, there is a semibridging CO ligand in **1-B** resulting in the nonlinear Fe(2)−C(15)−O(3) {157.7(5)°} arrangement with a short Fe−CO distance {Fe(1)−C(15): 2.450(6)

(15) Examples of CO stretching band of semibridging CO ligands: (a) Fe−C−O 163.2°, ν_{CO} = 1895 cm^{-1}: Fischer, E. O.; Winkler, E.; Huttner, G.; Regler, D., *Angew. Chem.* **1972**, *84*, 214. Huttner, G.; Regler, D. *Chem. Ber.* **1972**, *105*, 2726. (b) Fe−C−O 158.5°, ν_{CO} = 1884 cm^{-1}: Singh, K.; McWhinnie, W. R.; Chen, H. L.; Sun, M.; Hamor, T. A., *J. Chem. Soc., Dalton Trans.* **1996**, 1545.

(16) (a) Cotton, F. A.; Hunter, D. L.; Lahuerta, P. *J. Am. Chem. Soc.* **1975**, *97*, 1046. (b) Cotton, F. A.; Hunter, D. L. *J. Am. Chem. Soc.* **1975**, *97*, 5739. (c) Cotton, F. A.; Hunter, D. L.; Lahuerta, P. *Inorg. Chem.* **1975**, *14*, 511.

(17) As reported by Cotton and co-workers **1-A** showed three ^{13}C resonances due to the CO ligands in a ratio of 2:2:1 at −80 °C. On warming, two of them were coalesced and two signals (intensity = 2:3) appeared at 60 °C.[16c] In ^1H NMR spectra of **2-A**, five signals were seen at −60 °C. When the solution was warmed, three of them were broadened and disappeared. At 50 °C two sharp and one broad peak were observed in a ratio of 1:1:3. Only three signals were visible in a ratio of 1:3:1 from −80 °C to room temperature in the spectra of **2-B**. All of these results suggested that the CO exchange processes of **1-B** or **2-B** were much faster than those of **1-A** or **2-A**. Details are described in the Supporting Information.

Table 2. Crystallographic Data for 1-A, 1-B, 2-A, and 2-B

	1-A[e]	**1-B**	**2-A**	**2-B**
empirical formula	$C_{17}H_8Fe_2O_5$	$C_{17}H_8Fe_2O_5$	$C_{21}H_{10}Fe_2O_5$	$C_{21}H_{10}Fe_2O_5 \cdot 1/2\ C_6H_6$
fw	403.94	403.94	454.00	493.05
temp, K	293(2)	173(2)	296(2)	223(2)
radiation	Mo Kα (0.71069 Å)	Mo Kα (0.71069 Å)	Mo Kα (0.71069 Å)	Mo Kα (0.71069 Å)
cryst syst	orthorhombic	triclinic	orthorhombic	monoclinic
space group	$C222_1$	$P\bar{1}$	$Pccn$	$P2_1/n$
a, Å	12.781(1)	7.982(2)	16.790(4)	12.752(2)
b, Å	13.825(1)	12.874(2)	15.803(4)	11.951(2)
c, Å	16.792(1)	7.815(2)	13.351(3)	13.492(2)
α, deg	90	100.420(9)	90	90
β, deg	90	111.648(9)	90	103.053(10)
γ, deg	90	88.591(12)	90	90
V, Å^3	2967.3(4)	733.2(2)	3542.7(15)	2003.1(5)
Z	8	2	8	4
D_{calcd}, Mg/m^3	1.808	1.830	1.480	1.635
abs coeff, mm^{-1}	1.980	2.003	1.670	1.483
F(000)	1616	404	1824	996
cryst size, mm	0.35 × 0.30 × 0.20	0.30 × 0.30 × 0.25	0.20 × 0.20 × 0.10	0.50 × 0.40 × 0.20
θ range, deg	2.17 to 27.47	1.61 to 27.46	1.78 to 27.49	2.62 to 27.50
no. of indep reflns	1807 [R(int) = 0.0000]	3061 [R(int) = 0.0000]	2699 [R(int) = 0.0000]	4608 [R(int) = 0.0597]
no. of reflns obsd	1614 (>2σ)	2505 (>2σ)	2277 (>3σ)	2702 (>2σ)
refinement method	full-matrix least-squares on F^2	full-matrix least-squares on F^2	full-matrix least-squares on F	full-matrix least-squares on F^2
no. of data/restraints/params	1614/0/249	2505/0/218	2277/0/278	2702/0/332
goodness-of-fit[a] on F^2	1.063	1.128		1.006
final R indices [I>2σ(I)][b]	$R_1 = 0.0332$[b]	$R_1 = 0.0533$[b]	$R = 0.0560$[b,f]	$R_1 = 0.0417$[b]
	$wR_2 = 0.0745$[c]	$wR_2 = 0.1350$[c]	$R_w = 0.0320$[d,f]	$wR_2 = 0.1109$[c]
R indices (all data)[c]	$R_1 = 0.0386$[b]	$R_1 = 0.0696$[b]		$R_1 = 0.1147$[b]
	$wR_2 = 0.0766$[c]	$wR_2 = 0.1543$[c]		$wR_2 = 0.1336$[c]
larg diff peak & hole, e Å^{-3}	0.538 and −0.814	0.520 and −0.647	0.080 and −0.0235	0.827 and −0.503

[a] GOF = $[\sum w(F_o^2 - F_c^2)^2/(N - P)]^{1/2}$. [b] $R(F) = \sum||F_o| - |F_c||/\sum|F_o|$. [c] $wR(F_2) = [\sum w(F_o^2 - F_c^2)^2/\sum w(F_o^2)^2]^{1/2}$. [d] $R_w = [\sum w(|F_o| - |F_c|)^2/\sum wF_o^2]^{1/2}$. [e] The data were slightly different from the crystallographic data reported by Churchill and co-workers.[9] [f] $I > 3\sigma(I)$.

Table 3. Representative Bond Distances (Å) and Angles (deg) for 1-A

Fe(1)−Fe(2)	2.7702(9)	C(3)−C(4)	1.350(11)
Fe(1)−C(η^5)[a]	2.104 ± 0.024	C(4)−C(5)	1.449(10)
Fe(2)−C(5)	2.227(5)	C(5)−C(12)	1.407(7)
Fe(2)−C(12)	2.058(5)	C(12)−C(6)	1.434(8)
Fe(2)−C(6)	2.247(5)	C(6)−C(7)	1.445(8)
terminal CO		C(7)−C(8)	1.360(8)
Fe−C[a]	1.770 ± 0.018	C(8)−C(9)	1.438(8)
ligand		C(11)−C(12)	1.416(6)
C(10)−C(3)	1.432(9)		
Fe(1)−C(11)−C(12)	118.2(3)	Fe(2)−C(12)−C(11)	99.8(3)

[a] Average.

Table 4. Representative Bond Distances (Å) and Angles (deg) for 1-B

Fe(1)−Fe(2)	2.8042(11)	ligand	
Fe(1)−C(η^5)[a]	2.127 ± 0.073	C(10)−C(3)	1.441(7)
Fe(2)−C(3)	2.156(5)	C(3)−C(4)	1.400(8)
Fe(2)−C(4)	2.057(5)	C(4)−C(5)	1.429(8)
Fe(2)−C(5)	2.179(5)	C(5)−C(12)	1.460(7)
terminal CO		C(12)−C(6)	1.387(7)
Fe−C[a]	1.775 ± 0.025	C(6)−C(7)	1.431(9)
bridging CO		C(7)−C(8)	1.371(9)
Fe(1)−C(15)	2.450(6)	C(8)−C(9)	1.431(8)
Fe(2)−C(15)	1.813(5)	C(11)−C(12)	1.409(7)
O(3)−C(15)−Fe(2)	157.7(5)	Fe(1)−Fe(2)−C(4)	104.0(2)

[a] Average.

Å}. The Fe−Fe bond {2.8042(11) Å}of **1-B** is slightly longer than that of **1-A** {2.7702(9) Å}.

The complexes **2-A** and **2-B** have structures similar to **1-A** and **1-B**, respectively. Representative bond angles and distances are summarized in Tables 5 and 6. In both **2-A** and **2-B**, the aceanthrylene ligand is nonplanar. A striking difference in the structure of **2-B** versus **1-B** is the lack of a bridging CO ligand. The reason only **1-B** has a semibridging CO ligand is not clear at present.

Table 5. Representative Bond Distances (Å) and Angles (deg) for 2-A

Fe(1)−Fe(2)	2.782(1)	C(5)−C(12)	1.415(11)
Fe(1)−C(η^5)[a]	2.104 ± 0.019	C(12)−C(6)	1.419(10)
Fe(2)−C(5)	2.255(8)	C(6)−C(7)	1.471(10)
Fe(2)−C(12)	2.050(7)	C(7)−C(8)	1.414(10)
Fe(2)−C(6)	2.211(7)	C(8)−C(9)	1.459(9)
terminal CO		C(7)−C(18)	1.401(10)
Fe−C[a]	1.764 ± 0.028	C(18)−C(19)	1.365(12)
ligand		C(19)−C(20)	1.383(12)
C(10)−C(3)	1.435(12)	C(20)−C(21)	1.370(11)
C(3)−C(4)	1.346(13)	C(21)−C(8)	1.390(10)
C(4)−C(5)	1.446(12)	C(11)−C(12)	1.427(10)
Fe(1)−C(11)−C(12)	117.6(5)	Fe(2)−C(12)−C(11)	100.6(5)

[a] Average.

Table 6. Representative Bond Distances (Å) and Angles (deg) for 2-B

Fe(1)−Fe(2)	2.8182(8)	C(5)−C(12)	1.460(5)
Fe(1)−C(η^5)[a]	2.108 ± 0.044	C(12)−C(6)	1.348(6)
Fe(2)−C(3)	2.149(4)	C(6)−C(7)	1.450(6)
Fe(2)−C(4)	2.052(4)	C(7)−C(8)	1.416(6)
Fe(2)−C(5)	2.203(4)	C(8)−C(9)	1.456(5)
terminal CO		C(7)−C(18)	1.401(5)
Fe−C[a]	1.771 ± 0.016	C(18)−C(19)	1.377(7)
ligand		C(19)−C(20)	1.399(7)
C(10)−C(3)	1.443(6)	C(20)−C(21)	1.376(6)
C(3)−C(4)	1.383(7)	C(21)−C(8)	1.397(6)
C(4)−C(5)	1.440(7)	C(11)−C(12)	1.427(5)
O(3)−C(15)−Fe(2)	170.3(4)	Fe(1)−Fe(2)−C(4)	102.6(1)

[a] Average.

Thermal Haptotropic Isomerization of 1-B to 1-A and of 2-B to 2-A. As described above, the diiron complexes **1-A** and **2-A** were isolated as crystals. A ^{1}H NMR spectrum of **1-A** in a C_6D_6 solution under exclusion of light showed that the solution contained only **1-A**. After the solution stood in the dark for 24 h at room temperature, 2% of **1-A** was converted to **1-B**. Similarly,

Table 7. Kinetic Parameters for the Thermal Isomerization of 1 and 2

	1-B → 1-A	**2-B → 2-A**
$\Delta H^{\ddagger}_{298}$ (kcal mol^{-1})	23 ± 1	26 ± 1
$\Delta S^{\ddagger}_{298}$ (cal mol^{-1}deg^{-1})	1 ± 4	0 ± 2
$\Delta G^{\ddagger}_{298}$ (kcal mol^{-1})	23 ± 1	26 ± 1

a 98:2 mixture of **1-A** and **1-B** was obtained when a C_6D_6 solution of 100% pure **1-B** stood in the dark at room temperature for 24 h. These experiments suggest that **1-A** is essentially in equilibrium with **1-B**, but the equilibrium is in favor of **1-A**. The equilibrium constant is not very dependent on the temperature [K_{eq} = [**1-B**]/[**1-A**] = 0.021 (296 K), 0.027 (313 K), 0.035 (353 K)], from which $\Delta G°_{296}$ was estimated to be 2.3 kcal/mol. Formation of **2-B** was not detected in similar NMR measurements of **2-A** at a temperature range from room temperature to 60 °C, but **2-B** was completely converted to **2-A** by heating it in toluene-d_8 for 6 h at 87 °C. This can be attributed to the fact that **2-A** is also essentially in equilibrium with **2-B**, but $\Delta G°$ between **2-A** and **2-B** is too large to detect **2-B** in NMR.

The reaction from **1-B** to **1-A** proved first-order in the concentration of **1-B** until the fourth half-life. Since K_{eq} is small, the kinetics analysis was carried out for an irreversible first-order reaction.[18] From the temperature dependence of the rate constants [$k_{obs} \times 10^5$/s^{-1}; 0.46 ± 0.03 (281 K); 1.8 ± 0.2 (289 K); 5.4 ± 0.6 (297 K); 14.3 ± 1.2 (305 K); 36.8 ± 4.8 (313 K)] the values for $\Delta G^{\ddagger}_{298}$, $\Delta H^{\ddagger}_{298}$, and $\Delta S^{\ddagger}_{298}$ were obtained as 23 ± 1 kcal/mol, 23 ± 1 kcal/mol, and 1 ± 4 cal/mol·deg, respectively. Kinetic analysis of **2-B** gave rate constants ($k \times 10^5$/s^{-1}) of 2.3 ± 0.2 (333 K), 9.0 ± 0.5 (344 K), 20 ± 1 (351 K), and 46 ± 2 (360 K), from which were obtained $\Delta G^{\ddagger}_{298}$ = 26 ±1 kcal/mol, $\Delta H^{\ddagger}_{298}$ = 26 ± 1 kcal/mol, and $\Delta S^{\ddagger}_{298}$ = 0 ± 2 cal/mol·deg. The activation energy of the reaction of **2-B** is 3 kcal/mol higher than that of **1-B** (Table 7).

The haptotropic rearrangement of several mononuclear metal carbonyls bound to polyaromatic hydrocarbons has been subjected to kinetic analysis previously.[5] $\Delta H^{\ddagger}$ of these haptotropic rearrangements has been found to be 25−30 kcal/mol, whereas $\Delta S^{\ddagger}$ has been reported to be almost zero. The activation enthalpy of the isomerization from **1-B** to **1-A** or **2-B** to **2-A** is in accord with those reported. The small entropy change seen in many haptotropic rearrangements is indicative of small structural changes in the transition states versus the starting materials (vide infra).

The longer Fe−Fe bond is indicative of a weakening of the Fe−Fe bond. This leads to a more facile reduction of the Fe−Fe bond and actually results in a positive shift of reduction potentials of **1-B** and **2-B**, as determined by cyclic voltammetry, when compared to those of **1-A** and **2-A**, respectively. The cyclic voltammetric measurements were performed in acetonitrile with a scan rate of 100 mV/s. To avoid the effect of moisture and air, all of the measurements were carried out in a glovebox. All

(18) One may consider that the reaction from **1-B** to **1-A** should be treated with the reversible first-order kinetics which contain thermal equilibrium between **1-A** and **1-B**. We also calculated the activation parameters in the reversible first-order kinetics; $\Delta G^{\ddagger}_{298}$ = 24 ± 1 kcal/mol, $\Delta H^{\ddagger}_{298}$ = 23 ± 1 kcal/mol, $\Delta S^{\ddagger}_{298}$ = 2 ± 5 cal/mol·deg for the reaction **1-B** to **1-A**, which are in agreement with those obtained by the first-order kinetics shown in the text. Details are reported in the Supporting Information.

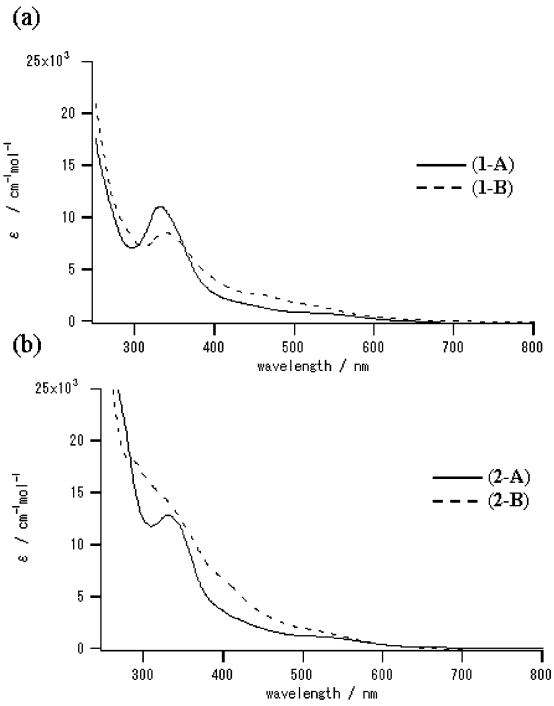

Figure 2. UV absorption spectra of **1** and **2**: (a) **1-A** and **1-B**, (b) **2-A** and **2-B**.

of the compounds provided an irreversible reduction wave, of which reduction potentials are −1.61 V (**1-A**), −1.38 V (**1-B**), −1.66 V (**2-A**), and −1.36 V (**2-B**). The shifts of the reduction wave of **1-B** and **2-B** toward more positive potentials compared with those of **1-A** and **2-A** indicate a lowering of the LUMO energies, which is supported by the EHMO calculations of **1-A** and **1-B**, as will be described later. The shift is also in accord with the longer Fe−Fe bonds in **1-B** (2.8042(11) Å) and **2-B** (2.8182(8) Å) as compared to those of **1-A** (2.7702(9) Å) and **2-A** (2.782(1) Å). Interestingly, there is only a slight difference in the reduction potentials of **1-A** and **2-A** and of **1-B** and **2-B**.

Photochemical Haptotropic Isomerization of 1-A to 1-B and 2-A to 2-B. The wavelength dependency of the photoisomerization was determined by photoirradiation of a toluene-d_8 solution of **1-A** using UV interference filters. To avoid concomitant thermal isomerization, the measurement was carried out at −78 °C. The isomer ratios at the photostatic state are **1-A**:**1-B** = 17:83, 12:88, and 9:91 at λ = 360 ± 10, 450 ± 10, and 600 ± 10 nm. Similar experiments of **2-A** provided the isomer ratios of **2-A**:**2-B** at the photostatic state as 66:34 (600 ± 10 nm), 68:32 (450 ± 10 nm), and 91:9 (360 ± 10 nm). In both of the photochemical reactions, a favorable formation of the thermodynamically unstable isomer was observed upon visible-light irradiation. This is similar to the observed wavelength dependency on the isomer ratios at the photostatic state for (μ_2,η^3:η^5-guaiazulene)$M_2(CO)_5$.

As shown in Figure 2, the UV−vis spectra of **1-A** and **1-B** in cyclohexane are similar to those of **2-A** and **2-B**, respectively. The quantum yields of the photoreactions of **1-A** or **1-B** (λ = 398 ± 10 nm) were determined by time-dependent UV−vis spectra as summarized in Table 9. Estimated quantum yields are $\Phi_{\mathbf{1-A\rightarrow 1-B}} > \Phi_{\mathbf{1-B\rightarrow 1-A}}$ and $\Phi_{\mathbf{2-A\rightarrow 2-B}} > \Phi_{\mathbf{2-B\rightarrow 2-A}}$. Those of the aceanthrylene complexes are approximately 10−30 times smaller than

Table 8. Isomer Ratios of A and B at the Photostatic State[a]

	1-A:1-B	2-A:2-B
Xenon (long range)	5:95	66:34
600 nm	9:91	66:34
450 nm	12:88	68:32
360 nm	17:83	91:9

[a] Irradiated in toluene-d_8 at −78 °C. The ratios were determined by ^{1}H NMR.

Table 9. Quantum Yields[a]

reaction	quantum yield (Φ)
1-A → **1-B**	0.30(3)
1-B → **1-A**	0.09(1)
2-A → **2-B**	0.013(2)
2-B → **2-A**	0.009(1)

[a] Irradiated in cyclohexane at λ = 398 nm. Change of the concentration of **1-A** and **1-B** or **2-A** and **2-B** was determined by UV−visible spectra.

those of the acenaphthylene compounds. Several studies have been published which include the quantum yields of organometallic photoisomerizations;[3b,e,19] the largest quantum yields (0.13−0.17) in the literature were observed for the isomerization of (μ_2,η^5:η^5-bicyclopentadienyl)$Ru_2(CO)_4$ to (μ_2,η^1:η^5-cyclopentadienyl)$_2Ru_2(CO)_4$ by Vollhardt and co-workers.[3b] The quantum yield of 0.30 in the reaction from **1-A** to **1-B** is larger than that of the Vollhardt complex.

Mechanistic Consideration with the Aid of Theoretical Studies. Albright and Hoffman carried out theoretical studies on the haptotropic rearrangement of (η^6-naphthalene)$Cr(CO)_3$ and proposed that the coordination site of the $Cr(CO)_3$ species moves intramolecularly from one six-membered ring (**A**; η^6-) to the other (**A′**; η^6-) through **B** (η^4-), **C** (η^3-), and **B′** (η^4-). From the potential energy surface calculated for shifting the $Cr(CO)_3$ species on the naphthalene ring, it could be determined that **B** and **B′** are transition states, 27 kcal/mol less stable than the ground states (**A** and **A′**), whereas **C** is a stationary point of 20 kcal/mol less stability. Reinvestigation of this rearrangement by DFT calculations showed a trimethylene methane-like transition state **D**, 30 kcal/mol less stable than the ground state.[5j] These and other theoretical studies are in good agreement with the experimental data of the haptotropic rearrangement discussed with $\Delta H^‡$ = 20−30 kcal/mol and $\Delta S^‡$ = ca. 0 cal/mol·deg. Thermal haptotropic rearrangement between **1-A** and **1-B** and that between **2-A** and **2-B** also proceed with $\Delta H^‡$ = 20−30 kcal/mol and $\Delta S^‡$ = ca. 0 cal/mol·deg as described above. This may indicate that the thermal reactions of the diiron compounds are mechanistically similar to the haptotropic shifts of $Cr(CO)_3$ species on the naphthalene ring.[20] A simplified MO diagram of **1-A** is illustrated in Figure 3, in which the interaction of occupied orbitals of the acenaphthylene dianion with unoccupied orbitals of $[Fe_2(CO)_5]^{2+}$ produces four frontier orbitals, NXHOMO, HOMO, LUMO, and NXLUMO, the former two of which are the dominant bonding orbitals.

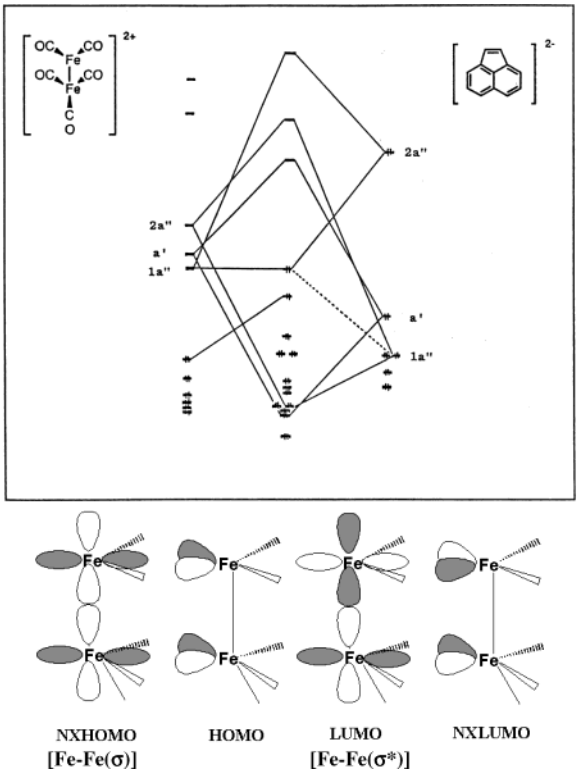

Figure 3. MO diagram of **1-A**.

Scheme 4

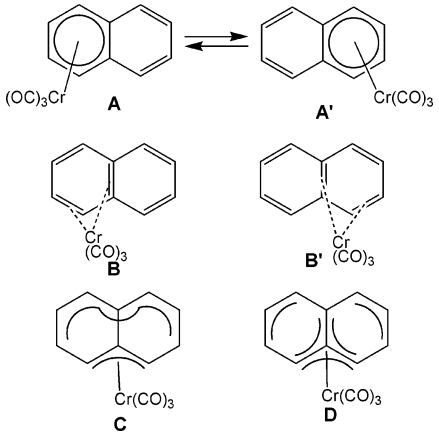

As shown in Figure 4, the haptotropic shift of **1-A** occurs such as that the $Fe(CO)_3$ group pivots on the iron center of the $Fe(CO)_2$ moiety. The EHMO calculations were carried out in keeping a distance between the acenaphthylene and the diiron species of 1.90 Å, indicating that the pivot turn proceeds through a transition state (θ = 20°). The activation energy of 25 kcal/mol is coincident with the experimental data.[21] In the transition state, the $Fe(CO)_3$ moiety is considered to be in the η^1-coordination mode, and a change of the coordination mode from one η^3-coordination to the other via a η^1-coordination governs the thermal haptotropic interconversion. Although there is no substantial difference in energy between the two haptotropic isomers in the

(19) Bruce, A. E.; Tyler, D. R. *Inorg. Chem.* **1984**, *23*, 3433.

(20) In earlier studies on the haptotropic rearrangement, mechanisms involving intermolecular exchange of the metal fragment are sometimes proposed.[6b] We carried out the rearrangement between **1-A** and **1-B** in the presence of aceanthrylene and that between **2-A** and **2-B** in the presence of acenaphthylene. In both of the experiments, no scrambling of the aromatic ring took place. We consider that this is good support for ruling out the intermolecular mechanism.

(21) EHMO calculations were performed on a PC version of the EHMO program purchased from Kodansha Scientific, Ltd.: Details are described in the Supporting Information.

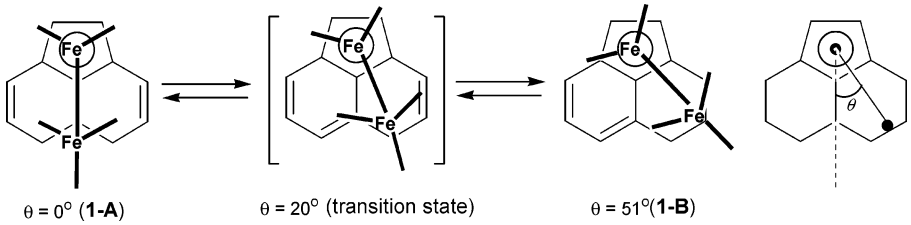

Figure 4. Pivot turn of the Fe_2 species in **1**.

EHMO calculations, the reason why **1-B** is less thermodynamically stable than **1-A** could be attributed to Churchill's proposal that the η^3-coordination of the acenaphthylene ligand to the $Fe(CO)_3$ moiety in **1-B** makes the Fe−Fe distance longer than in **1-A** and longer than usual Fe−Fe bonds in many other diiron complexes. In fact, the Fe−Fe bond distances determined from X-ray crystal structure are longer by 0.03−0.04 Å in **1-B** and **2-B** than in **1-A** and **2-A**, respectively.

The elongation of the Fe−Fe bond by the haptotropic shift from **1-A** (or **2-A**) to **1-B** (or **2-B**) may be related to the mechanisms of photochemical haptotropic rearrangement. It is likely that photolysis of the diiron compounds leads to a $\sigma \rightarrow \sigma^*$ transition (NXHOMO → LUMO), which makes the Fe−Fe bond weaker. EHMO calculations of **1-A** and **1-B** suggest that the overlap populations of both Fe−Fe and Fe(2)−η^3-allyl bonds become smaller in the LUMO than those in the NXHOMO; this causes an elongation of the Fe−Fe bond and a facile haptotropic shift.[22] Thus, photoirradiation of **1-A** and **1-B** could produce the corresponding excited states, **1-A*** and **1-B***, which are interconverted facilely in keeping the Fe−Fe bond longer than in the ground states. The longer Fe−Fe bond is favorable for **1-B***; this results in predominant formation of **1-B**.

There are several notable differences in the interconversion of the two haptotropic isomers in the acenaphthylene and aceanthrylene complexes: In the thermal rearrangement, the energy difference between **2-A** and **2-B** ($\Delta G°$) and the activation energy of the rearrangement ($\Delta G^‡$) are larger than those in the interconversion of **1-A** and **1-B**. In contrast, the isomer ratio in the photostatic state of **2-A**/**2-B** is not significantly in favor of **2-B**, whereas the quantum yield for the photochemical conversion of **2-A** to **2-B** is 1 order of magnitude smaller than those for the formation of **1-B** from **1-A**. The quantum yield for the formation of **1-B** from **1-A** ($\Phi_{A\rightarrow B} = 0.30$) is much larger than that reported for other organometallic complexes showing thermally reversible photoisomerization behavior ($\Phi < 0.17$).[3b,e,19] The benzene ring in the aceanthrylene ligand apparently dissipates the photoenergy. Further investigation is required to understand these differences; it is worthwhile to point out that they may be related to differences in the structural features of the acenaphthylene and aceanthrylene ligands. Thus, one explanation for the higher $\Delta G^‡$ may be that the benzene ring of the aceanthrylene ligand reduces the flexibility of the π-ligand required for the $\eta^3 \rightarrow \eta^1 \rightarrow \eta^3$ interconversion. Two possible interpretations for the lower quantum yields are (1) the benzene ring of the aceanthrylene ligand may effectively quench the excited states, **2-A*** and **2-B***, and (2) there is an energy release pathway by luminescence from **2-A*** or **2-B***, which is not observed in the acenaphthylene complexes.[23]

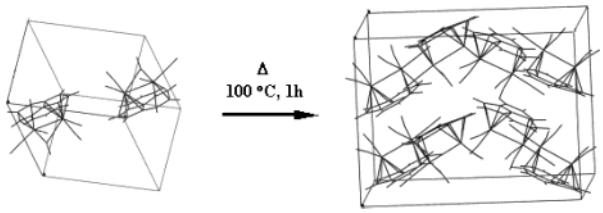

Figure 5. Thermal isomerization of **1** in a single crystal.

Thermal and Photochemical Isomerization of 1-B in the Solid State. The experimental results described above revealed that both the thermal ($\Delta G^‡ =$ 23 kcal/mol) and photochemical ($\Phi = 0.30$) haptotropic rearrangement take place with ease in solution. While photochromism in solution has been widely investigated, photochromism in the solid state[24] has lately attracted attention in relation to studies on molecular switches and crystal engineering.[2d,24] The possibility of thermally reversible photoisomerization of organometallic compounds was shown by Vollhardt and co-workers, who reported that thermal rearrangement from (μ_2,η^1:η^5-cyclopentadienyl)$_2Ru_2(CO)_4$ to (μ_2,η^5:η^5-bicyclopentadienyl)$Ru_2(CO)_4$ actually takes place in crystals.[3b] However, there has been no preceding paper on the solid state of organometallic compounds showing both the photochemical and thermal processes proceeding.

Our first challenge was the isomerization of **1-A** or **1-B** in a single crystal. Although photolysis of a crystal of **1-A** did not show any change, presumably due to its intense color, which prevented transmission of the light, heating of a crystal of **1-B** at 100 °C for 1 h eventually formed a single crystal of **1-A** (Figure 5 and Table 10).[25] Crystallography of a single crystal of **1-B** was carried out at −100 °C, and the lattice constants were determined to be $a = 7.982(2)$ Å, $b = 12.874(2)$ Å, $c = 7.815(2)$ Å, $\alpha = 100.420(9)°$, $\beta = 111.648(9)°$, $\gamma = 88.59(1)°$. Refinement was performed, and the molecular structure of **1-B** was confirmed with R1($I>2\sigma(I)$) = 0.053. This single crystal was heated at 100 °C for 1 h, and then a crystallographic analysis was carried out at −100 °C.

(22) DFT calculations of **1-A*** and **1-B*** support that photoirradiation put one electron into a σ^* orbital of the Fe−Fe bond: Mogi, K.; Niibayashi, S.; Matsubara, K.; Nagashima, H., to be published.

(23) Excitation of **2-A** (1×10^{-5} M in cyclohexane) at $\lambda = 340$ nm gave off luminescence of $\lambda = 491.5$ nm, the intensity of which was 4.1 $\times 10^2$. Under the same conditions aceanthrylene gave off luminescence (intensity = 3.7×10^3), whereas no luminescence was observed for **1-A**.

(24) For recent studies: See the following literature and references therein. (a) Kobatake, S.; Yamada, T.; Uchida, K.; Kato, N.; Irie, M. *J. Am. Chem. Soc.* **1999**, *121*, 2380. (b) Ohashi, Y.; Yanagi, K.; Kurihara, T.; Sasada, Y.; Ohgo, Y. *J. Am. Chem. Soc.* **1981**, *103*, 5805. Ohashi, Y. *Acc. Chem. Res.* **1988**, *21*, 268. (c) Kawano, M.; Sano, T.; Abe, J.; Ohashi, Y. *J. Am. Chem. Soc.* **1999**, *121*, 8106. (d) Miller, E. J.; Brill, T. B.; Reingold, A. L.; Fultz, W. C. *J. Am. Chem. Soc.* **1983**, *105*, 7580. (e) Scheffer, J. R. *Acc. Chem. Res.* **1980**, *13*, 283.

(25) The lattice parameters of **1-A** reported by Churchill[9] are $a =$ 10.056(7) Å, $b = 16.089(10)$ Å, $c = 9.376(6)$ Å, $\alpha = 90°$, $\beta = 91.53(9)°$, and $\gamma = 90°$, $Z = 4$.

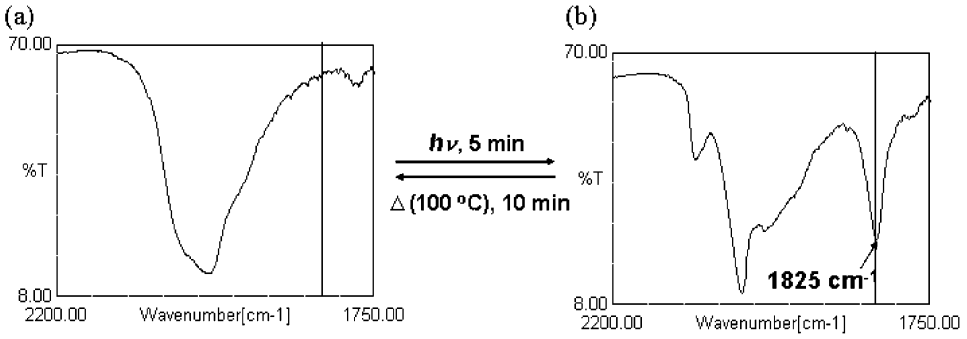

Figure 6. IR spectra of annealed **1-A** and **1-B** in KBr pellets.

Table 10. Crystallographic Data for the Thermal Isomerization of 1-B in the Same Single Crystal

	1-B	**1-A**[a,b]
a (Å)	7.982(2)	12.765(1)
b (Å)	12.874(2)	13.778(2)
c (Å)	7.815(2)	16.719(2)
α (deg)	100.420(9)	90
β (deg)	111.648(9)	90
γ (deg)	88.59(1)	90
V (Å^3)	733.2(2)	2940.3(5)
Z	2	8
ρ(calcd)	1.829	1.825
temp (K)	173	173
space group	$P\bar{1}$	$C222_1$
R1	0.053	0.040

[a] A single crystal obtained by heating of a single crystal of **1-B**. [b] The crystallographic data are coincident with that of **1-A** (see Table 2).

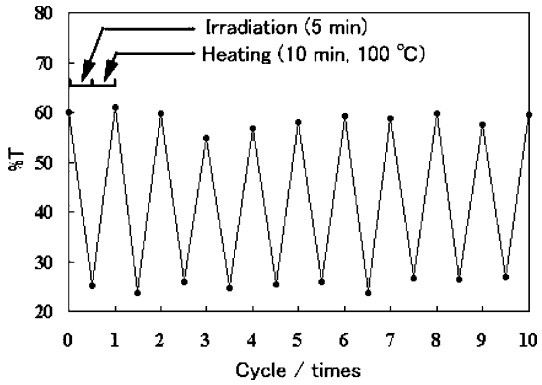

Figure 7. Photolysis (5 min)/thermal treatment (100 °C, 10 min) cycles detected by reversible change of transmissions at $\nu = 1825$ cm^{-1}.

The lattice parameters had changed to $a = 12.765(1)$ Å, $b = 13.778(2)$ Å, $c = 16.719(2)$ Å, $\alpha = 90°$, $\beta = 90°$, $\gamma = 90°$, and the refinement provided the molecular structure of **1-A** with R1($I>2\sigma(I)$) = 0.040. During this process, the density of the crystal did not change.

That a photochemical rearrangement of **1-A** did not occur in the single crystal is due to an inefficient transmission of the light; therefore, we next examined the photoisomerization of **1-A** to **1-B** and its reverse thermal reaction using a solid sample dispersed in a KBr disk as used for IR measurements. As described above, **1-B** has a semibridging CO ligand showing a characteristic ν_{CO} band in the IR spectrum. This absorption serves as a good indicator for the formation of **1-B**. The pellets were prepared from 0.5 mg of **1-A** (or **1-B**) and KBr (30 mg). The IR spectra of the disk containing **1-A** just after the preparation exhibited several ν_{CO} bands due to the individual CO ligands. Photolysis of this disk for 10 h with a 500 W xenon lamp gave the IR spectrum shown in Figure 6b, in which sharp bands at 1825, 2016, and 2083 cm^{-1} are visible (IR-B). Similarly, the initial IR spectrum of the disk containing **1-B** showed several ν_{CO} bands including a 1856 cm^{-1} band due to the individual CO ligands. Heating of this disk at 100 °C for 1 h gave the IR spectrum shown in Figure 6a, in which only broad absorptions around 1982 cm^{-1} were visible (IR-A). It is important that the disk showing IR-A gives the spectrum identical to IR-B within minutes upon photolysis. Similarly, the disk showing IR-B was heated at 100 °C and afforded the IR spectrum identical to IR-A. Thus, the photolysis (5 min)/thermal treatment (10 min at 100 °C) cycle provided a reversible change of the IR spectrum of the disk between IR-A and IR-B, which could be repeated more than 10 times without change in the signal intensity as shown in Figure 7. The initial thermal treatment of the disk containing **1-B** as well as the initial photochemical treatment of the disk of **1-A**, both of which required a relatively long time until the IR spectrum remained unchanged, induces annealing and thus causes the diiron complexes in the disk to reach a stationary state.[26] After annealing, a short photochemical or thermal treatment is enough to provide the reversible change in the IR spectra by the photolysis/thermal treatment cycle as described above. The disk showing IR-A after several photolysis/thermal treatment cycles was subjected to extraction of the diiron complex by CH_2Cl_2. The NMR spectrum of the diiron complex so obtained is identical to an authentic sample of **1-A**. Similar experiments with the disk showing IR-B revealed the diiron component in the disk to be **1-B**. Thus, thermally reversible photoisomerization between **1-A** and **1-B** definitely takes place in the KBr disk without decomposition of the diiron compounds under the above conditions.

Conclusion

As described above, the results presented in this paper revealed the thermally reversible photoisomerization behavior of diiron carbonyl complexes bound to acenaphthylene or aceanthrylene in both the solution and the solid state, providing the following important new aspects of the haptotropic rearrangement: (1)

(26) Annealing of the pellets containing **1-A** and **1-B** resulted in a significant change of their IR spectra (IR-A and IR-B, respectively). Conversion of microcrystalline to amorphous may cause this change, which is promoted by photolysis of **1-A** or thermal treatment of **1-B**.

Detailed studies on the preparation, structural analysis, and thermally reversible photoisomerization of (μ_2,η^3:η^5-acenaphthylene)$Fe_2(CO)_5$ were carried out, which showed a significant difference (98:2 vs 5:95 in solution) in the isomer ratio between the thermal and photochemical processes. This is a notable feature in comparison with small differences in the isomer ratios between the two processes observed in the thermally reversible photoisomerization of diiron or diruthenium carbonyl complexes bound to guaiazulene.[10] (2) Two isomers of the novel aceanthrylene homologue were synthesized and subjected to studies on their molecular structures, spectral properties, and thermal and photochemical haptotropic rearrangement behavior. The isomer ratios in the thermal and photochemical processes are different from those of the acenaphthylene homologue. (3) The photochemical haptotropic rearrangement of the acenaphthylene and aceanthrylene complexes, including the wavelength dependency and the determination of the quantum yields, was investigated. Kinetic studies on the thermal rearrangements provided the thermodynamic parameters of the rearrangements. It is noteworthy that the quantum yields of the acenaphthylene complex are significantly higher as compared to other organometallic photoswitches, whereas the thermodynamic parameters are roughly coincident with those reported for other haptotropic rearrangements. From these results, the reaction mechanisms were discussed with the aid of EHMO calculations. This contributes to our understanding of the poorly investigated photochemical haptotropic rearrangement. (4) The haptotropic rearrangement in the solid state resulted in bringing about a successful thermal isomerization from **1-B** to **1-A** in a single crystal and a thermally reversible photoisomerization between **1-A** and **1-B** in a KBr pellet.

The fourth point is of particular interest: the isomerization was detected by IR spectroscopy. The isomerization read out by nondestructive methods is a topic in recent organic photochromisms which may open the way to the development of practical devices,[2d] and the present results are the first example of organometallic photochromisms in the solid state detectable by IR light.

Experimental Section

General Procedures. All experiments were carried out under an argon atmosphere using standard Schlenk techniques. Ether, THF, benzene, toluene, heptane, hexane, and benzene-d_6 were distilled from benzophenone ketyl and stored under an argon atmosphere. Purification of acenaphthylene was performed by column chromatography followed by recrystallization. Other reagents and solvents were used as received. The ^{1}H NMR spectra were taken with a JEOL Lambda 400 or 600 spectrometer. Chemical shifts were recorded in ppm from the internal standard (^{1}H, ^{13}C: solvent). IR spectra were recorded in cm^{-1} on a JASCO FT/IR-550 spectrometer. The iron complexes **1-A** and **1-B** were prepared according to published methods.[8] Photoirradiation was carried out with a Ricoh 450 or 500 W high-pressure Hg lamp or an Ushio 500 W xenon lamp.

Preparation of 1-A. Slight modification from the literature procedure of the preparative process of **1-A** was made:[14] Into a 200 mL round-bottom flask fitted with a reflux condenser, $Fe_3(CO)_{12}$ (6.90 g, 13.7 mmol) and acenaphthylene (2.83 g, 18.6 mmol) were placed, and the atmosphere was replaced by nitrogen. Benzene (91 mL) was added to the flask, and the resulting suspension was heated under reflux for 10 h. After the mixture was cooled to room temperature, a black precipitate was filtered off by passing the mixture through a short pad of Celite. The solvent was removed in vacuo, and the residue was extracted with dichloromethane. Then Celite (ca. 2 g) was added to this solution and stirred for 1 min. After concentration, the residue was moved to the top of an Al_2O_3 column (20 mm ϕ × 100 mm). Elution with a 1:4 mixture of ether and *n*-hexane gave a yellow band containing acenaphthylene. A second red-brown band containing **1-A** was obtained by eluting with a 2:1 mixture of ether and *n*-hexane. Recrystallization of chromatographically purified **1-A** from a mixture of benzene and *n*-pentane gave analytically pure **1-A** in 32% yield (1.10 g). Mp: (dec) 152−153 °C. ^{1}H NMR ($CDCl_3$, rt): δ 6.19 (dd, J = 6.05, 8.98 Hz, 2H, H4), 6.09 (d, J = 8.98 Hz, 2H, H3), 5.65 (s, 2H, H2), 4.76 (d, J = 6.05 Hz, 2H, H5). ^{13}C{^{1}H} NMR ($C_6D_5CD_3$, −60 °C): δ 218.61 (2CO), 216.52 (2CO), 209.18(1CO). ^{13}C{^{1}H} NMR ($C_6D_5CD_3$, rt): δ 216.94 (CO), 129.45 (C4), 116.59 (C3), 91.94 (4°), 91.24 (4°), 87.19 (4°), 78.17 (C2), 58.26 (C5). IR (KBr, cm^{-1}): ν_{CO} 2025, 2017, 1964, 1950, 1921.

Preparation of 1-B. In a 5 mm ϕ glass tube, **1-A** (25 mg, 0.06 mmol) was dissolved in ether (1.5 mL). The sample was degassed, and then the tube was flame-sealed in a vacuum. After irradiation of this solution for 70 min using a 400 W high-pressure Hg lamp, the precipitate formed was filtered off. After careful addition of *n*-hexane to the filtrate the solution was allowed to stand at −78 °C for 1 day to give dark red crystals of **1-B** (18 mg, 72% with purity 95%). Anal. Calcd for $C_{12}H_8O_5Fe_2$: C, 50.55; H, 2.00. Found: C, 50.57; H, 1.92. Mp: (dec) 162−163 °C. ^{1}H NMR ($C_6D_5CD_3$, −15 °C): δ 6.18 (d, J = 8.43 Hz, 1H, H8), 6.14 (dd, J = 6.78, 8.43 Hz, 1H, H7), 5.47 (d, J = 6.41 Hz, 1H, H6), 5.27 (d, J = 5.31 Hz, 1H, H3), 4.96 (dd, J = 5.31, 6.41 Hz, 1H, H4), 4.31 (d, J = 1.28 Hz, 1H, H1), 3.29 (d, J = 1.28 Hz, 1H, H2), 2.49 (d, J = 6.41 Hz, 1H, H5). ^{13}C{^{1}H} NMR ($C_6D_5CD_3$, −80 °C, CO region): δ 220.87 (1CO), 216.68 (3CO), 215.83(1CO). ^{13}C{^{1}H} NMR ($C_6D_5CD_3$, −15 °C): δ 146.14 (4°), 131.78 (C7), 118.46 (C8), 114.07 (C6), 103.73 (4°), 87.28 (4°), 83.59 (C4), 79.64 (4°), 71.62 (C2), 71.56 (C1), 58.26 (C5), 57.53(C3); CO signals were not observed at this temperature. IR (KBr, cm^{-1}): ν_{CO} 2027, 1982, 1961, 1935, 1856.

Preparation of 2-A. Into a 50 mL round-bottom flask with a reflux condenser, $Fe_3(CO)_{12}$ (181 mg, 0.36 mmol) and aceanthrylene (62 mg, 0.30 mmol) were placed, and the atmosphere was replaced by nitrogen. *n*-Heptane (10 mL) was added to the flask, and the resulting suspension was heated for 2 h under reflux. After the mixture was cooled to room temperature, a black precipitate was filtered off by passing the mixture through a short pad of Celite. The solvent was removed in vacuo, and the residue was extracted with dichloromethane (5 mL). Then Celite (ca. 400 mg) was added to the solution, which was stirred for 1 min. After removal of the solvent in vacuo, the residue was moved to the top of the Al_2O_3 column (15 mm ϕ × 160 mm) at −15 °C, and elution with *n*-hexane gave a yellow band containing aceanthrylene. A second red-brown band containing **2-A** was obtained by eluting with a 1:1 mixture of ether and *n*-hexane. Recrystallization of chromatographically purified **2-A** from a mixture of ether and *n*-pentane gave analytically pure **2-A** in 34% yield (45.8 mg). Anal. Calcd for $C_{21}H_{10}O_5Fe_2$: C, 55.56; H, 2.22. Found: C, 55.41; H, 2.25. Mp: (dec) 155−160 °C. ^{1}H NMR ($CDCl_3$, rt) δ 7.41 (m, 1H, H7, H8, H9, or H10), 7.32 (m, 1H, H7, H8, H9, or H10), 7.21 (m, 2H, two of H7−H10), 6.33 (dd, J = 5.8, 9.2 Hz, 1H, H4), 6.26 (d, J = 9.2 Hz, 1H, H3), 5.92 (d, J = 2.9 Hz, 1H, H1), 5.77 (d, J = 2.9 Hz, 1H, H2), 4.89 (s, 1H, H6), 4.82 (d, J = 5.8 Hz, 1H, H5). ^{13}C{^{1}H} NMR ($C_6D_5CD_3$, −60 °C, CO region): δ 218.15 (1CO), 217.18 (1CO), 217.13 (1CO), 216.26 (1CO), 209.68 (1CO). ^{13}C{^{1}H} NMR ($CDCl_3$, rt): δ 216.81 (CO), 215.93 (CO), 134.99 (4°), 128.93 (C4), 128.01 (C7−C10), 127.86

(C7−C10), 126.77 (C7−C10), 125.10 (4°), 122.20 (C7−C10), 117.00 (C3), 89.42 (4°), 87.38 (4°), 87.15 (4°), 83.82 (4°), 78.84 (C2), 77.10 (C1), 56.82 (C6), 59.37 (C5). IR (KBr, cm^{-1}): ν_{CO} 2035, 1994, 1978, 1960, 1953.

Preparation of 2-B. In a 5 mm ϕ glass tube, **2-A** (20 mg, 0.04 mmol) was dissolved in ether (1.5 mL). The sample was degassed several times and sealed in a vacuum. After irradiation of this sample for 130 min using a 400 W high-pressure Hg lamp, the precipitate formed was filtrated off. After concentration of the reaction mixture, the residue was purified by column chromatography (silica, 15 mm ϕ × 400 mm, −15 °C) by eluting with *n*-hexane to give a yellow band containing aceanthrylene. A second red-brown band containing **2-A** and a third red-brown band containing **2-B** were obtained by eluting with a 10:1 mixture of *n*-hexane and ether. Removal of the solvent from the third band afforded **2-B** as a brown solid (1 mg, 5% with purity 95%). Decomposition of some amount of **2-B** during the chromatography caused a significant lowering in isolated yield. Analytically pure **2-B** was obtained by recrystallization from benzene/hexane. Anal. Calcd for $C_{21}H_{10}O_5Fe_2$: C, 55.55; H, 2.22. Found: C, 55.54; H, 2.24. Mp: (dec) 158−161 °C. ^{1}H NMR ($CDCl_3$, rt): δ 7.67 (m, 1H, H8−H10), 7.35 (m, 3H, H7−H10), 6.32 (s, 1H, H6), 5.90 (d, J = 5.8 Hz, 1H, H3), 5.80 (dd, J = 5.8, 6.5 Hz, 1H, H4), 5.54 (d, J = 2.7 Hz, 1H, H1), 4.26 (d, J = 2.7 Hz, 1H, H2), 3.71 (d, J = 6.5 Hz, 1H, H5). ^{13}C{^{1}H} NMR ($C_6D_5CD_3$, −80 °C, CO region): δ 220.23 (1CO), 216.57 (3CO), 215.41 (1CO). ^{13}C{^{1}H} NMR ($CDCl_3$, rt): δ 219.15 (1CO), 215.66 (3CO), 214.55 (1CO), 137.64 (4°), 135.16 (4°), 129.10 (C7−C10), 128.74 (C7−C10), 128.22 (C7−C10), 126.50 (4°), 124.47 (C8−C10), 114.67 (C6), 99.72 (4°), 84.92 (4°), 83.01 (C4), 81.17 (4°), 70.07 (C1), 69.83 (C2), 60.67 (C5), 54.67 (C3). IR (KBr, cm^{-1}): ν_{CO} 2022, 1920 (br).

X-ray Data Collection and Reduction. Single crystals of **1-A**, **1-B**, **2-A**, and **2-B** were grown from a mixture of ether and *n*-pentane. X-ray crystallography was performed on a Rigaku RAXIS RAPID imaging plate diffractometer (for **1-A** and **1-B**), a Rigaku AFC-5R four-cycle axis diffractometer (for **2-A**), or a Rigaku AFC-7R four-cycle axis diffractometer (for **2-B**) with graphite-monochromated Mo Kα radiation (λ = 0.71070 Å). The data were collected at 293(2) K (**1-A**), 173(2) K (**1-B**), 296(2) K (**2-A**), and 223(2) K (**2-B**) using ω scan in the θ range of 2.17° ≤ θ ≤ 27.48° and 1.61° ≤ θ ≤ 27.46° (**1-A** and **1-B**, respectively) and using the ω−2θ technique in the θ range of 1.78° ≤ θ ≤ 27.49° and 2.62° ≤ θ ≤ 27.50° (**2-A** and **2-B**, respectively). In the cases of **1-A**, **1-B**, and **2-B**, data collection and cell refinement were carried out using MSC/AFC Diffractometer Control on a Pentium computer. The structures were solved by the Patterson method (DIRDIF94 Patty)[27a] and were refined using full-matrix least squares (SHELXL97-2)[27b] based on F^2 of all independent reflections measured. In contrast, all calculations of **2-A** were performed with the UNICSIII program system (Sakurai and Kobayashi, 1979) on a HITAC M-680H at the Computer Center of the Institute for Molecular Science. The structure of **2-A** was solved by the Patterson method and expanded using Fourier techniques and was refined using full-matrix least-squares based on F of the observed reflections ($I > 3\sigma(I)$). All H atoms were located at ideal positions (**1-A**, **1-B**, and **2-B**), whereas those of **2-A** were located from difference Fourier maps. They were included in the refinement, but restricted to riding on the atom to which they were bonded in the cases of **1-A**, **1-B**, and **2-B**. Isotropic thermal factors of H atoms were held to 1.2−1.5 times (for methyl groups) U_{eq} of the riding atoms.

Photoisomerization of 1-A to 1-B and 2-A to 2-B. A solution of **1-A** or **2-A** (1 mg, 0.002 mmol) in toluene-d_6 (0.4 mL, 0.05 M) was sealed in a 5 mm ϕ tube in a vacuum. The solution was irradiated using a Xenon lamp with interference filters (360, 450, and 600 nm). The reactions were monitored periodically by ^{1}H NMR spectroscopy.

Kinetic Studies on the Thermal Isomerization of 1-B to 1-A and 2-B to 2-A. The reactions were conducted in a 5 mm ϕ NMR tube flame-sealed in a vacuum [solvent: C_6D_6, initial concentrations: 9.3×10^{-3} M (**1-B**) and 8.3×10^{-3} M (**2-B**)]. ^{1}H NMR spectra of **1-B** were measured at 281, 289, 297, 305, and 313 K in the NMR probe, where the temperatures were calibrated with a solution of ethylene glycol. Thermal treatment of **2-B** was carried out in an oil bath, of which the temperature was carefully controlled at 333, 344, 351, and 360 K, respectively. The sample was periodically cooled with a dry ice-acetone bath (−78 °C) and subjected to ^{1}H NMR measurement. Concentration of the products was determined by integral values [solvent signal (δ 7.15) was used as internal standard]. The data were treated in terms of first-order kinetics; plots of $-\ln([\mathbf{1\text{-}B}]/[\mathbf{1\text{-}B}]_0)$ [or $-\ln([\mathbf{2\text{-}B}]/[\mathbf{2\text{-}B}]_0)$] versus time resulted in straight lines ($r > 0.99$) ($[\mathbf{x}]_0$ = initial concentration; $[\mathbf{x}]$ = concentration at time t, where **x** is **1-B** or **2-B**). The rate constants k were extracted from the slopes of these lines. Plots of logarithmic function of the rate constants versus reciprocal of temperature gave typical Arrhenius plots, from which the activation parameters at 298 K were determined. The parameters of **1** were also calculated in terms of reversible first-order kinetics. They are almost the same as those calculated by first-order kinetics. Details are described in the Supporting Information.

Quantum Yield Measurements. Quantum yields for the photoisomerization of **1-A** to **1-B** or **2-A** to **2-B** were determined by UV−visible spectra. Actinometry was carried out just before the quantum yield measurement by the standard method using potassium ferrioxalatoiron(III) in water, resulting in 1.0×10^{-9} einstein/s for the measurement of **1-A** and 6.6×10^{-9} einstein/s for **2-A**. Reliability of these values was confirmed by measurement of quantum yields for the photooxidation of Cp_2Fe by CCl_4 to $[Cp_2Fe]Cl$ ($\Phi_{360\ nm} = 1.4$ in the literature[28a]). In a glovebox, solutions of **1-A** or **2-A**, dissolved in cyclohexane (1.0 or 1.3×10^{-4} mol L^{-1}), were placed in a quartz UV cell (1.0 cm) with a stopcock. The solutions were irradiated with a Xenon lamp with an interference filter (λ_{max} = 397.5 nm) for 30 min under a nitrogen atmosphere at room temperature. The UV−vis spectra were collected periodically during the irradiation, and only the initial stage of the data, in which the conversion of the diiron complex was less than 20%, was used for the calculation shown in Figures S-8-1 and 2. The conversion of **1-A** and **2-A** was determined by absorptions at λ = 331 nm (**1-A**) and λ = 400 nm (**2-A**), where there was the greatest difference in ϵ between the two haptotropic isomers ($\epsilon_{\mathbf{1-A}} = 10\,900$ vs $\epsilon_{\mathbf{1-B}} = 8350$, where $\lambda = 331$ nm; $\epsilon_{\mathbf{2-A}} = 3650$, $\epsilon_{\mathbf{2-B}} = 6760$, where $\lambda = 400$ nm). The quantum yields were determined to be $\Phi_{\mathbf{1A\rightarrow 1B}} = 0.30 \pm 0.03$, $\Phi_{\mathbf{1B\rightarrow 1A}} = 0.09 \pm 0.01$, $\Phi_{\mathbf{2A\rightarrow 2B}} = 0.013 \pm 0.002$, $\Phi_{\mathbf{2B\rightarrow 2A}} = 0.009 \pm 0.001$ according to Yokoyama's method.[28b]

Cyclic Voltammetry. Cyclic voltammetric studies were carried out using a BAS 50 B/W electrochemical analyzer in a glovebox. A platinum working electrode, a platinum wire counter electrode, and a silver reference electrode comprised of a silver wire in contact with 0.01 M $AgNO_3$ and 0.2 M $(^nBu)_4N^+PF_6^-$ in acetonitrile were used. The measurement was carried out in a THF solution of the sample (2×10^{-4} M) and $(^nBu)_4N^+PF_6^-$ (0.1 M used as the supporting electrolyte) in the presence of a small amount of ferrocene (internal standard). The scan rate was 0.1 V/s.

Thermal Isomerization of 1-B in a Single Crystal. A single crystal of **1-B** was sealed in a glass capillary under a nitrogen atmosphere, and the structure determination was

(27) (a) Beurskens, P. T.; Admiraal, G.; Beurskens, G.; Bosman, W. P.; de Gelder, R.; Israel, R.; Smits, J. M. M. *The DIRDIF-94 program system*, Technical Report of the Crystallography Laboratory; University of Nijmegen: The Netherlands, 1994. (b) Sheldrick, G. M. *SHELXL-97*; University of Göttingen: Germany, 1997.

(28) (a) Traverso, O.; Scandola, F. *Inorg. Chim. Acta* **1970**, *4*, 493. (b) Yokoyama, Y.; Kurita, Y. *Yuuki Gosei Kagaku* **1991**, *49*, 364.

performed on a Rigaku R-AXIS RAPID imaging plate diffractometer. After the measurement, the sample was heated in an oil bath at 100 °C for 1 h, and another crystallographic analysis was carried out to find the cell parameters of the crystal as well as bond lengths, and distances of the molecule were confirmed to be the same as those of **1-A**.[29]

Isomerization of 1 in a KBr Pellet. IR pellets of single crystals of **1-A** and **1-B**, respectively, in KBr were prepared under a N_2 atmosphere. Photolysis of the KBr pellets was performed with a 500 W xenon lamp under aerobic conditions. Heating of the KBr pellets was performed in an oil bath at 100 °C in a glass tube. After several photolysis/thermal treatment cycles, the KBr pellets were extracted with CH_2Cl_2. After removal of the solvent, the residue was subjected to spectroscopy to confirm that the diiron compound was not decomposed. The extraction just after the photolysis of the KBr pellets gave **1-B** as a single product, whereas that just after the thermal treatment afforded **1-A**, exclusively.

(29) We attempted to measure DSC for the determination of $\Delta G°$ under an inert gas atmosphere; however, two overlapping peaks barely assignable were observed.

Acknowledgment. A part of this study was financially supported by the Japan Society for the Promotion of Science (Grant-in-Aid for Scientific Research, 15036253 and 13450374).

Supporting Information Available: Methods of X-ray crystallography, the molecular structure and X-ray crystallographic data of **1-A**, **1-B**, **2-A**, and **2-B**, NMR spectra of **1-A**, **1-B**, **2-A**, and **2-B**, kinetic studies of the thermal isomerization of **1-B** or **2-B**, measurement of quantum yields, EHMO calculation of **1**, cyclic voltammetric studies, NMR spectra of **1-A**, **1-B**, **2-A**, and **2-B**, variable-temperature ^{13}C NMR spectra of **1-A**, **1-B**, **2-A**, and **2-B** in the CO region, and crystallographic data for the thermal isomerization of **1-B** in a single crystal. This material is available free of charge via the Internet at http://pubs.acs.org.

OM034117I